Hassallidin A, a Glycosylated Lipopeptide with Antifungal Activity from the Cyanobacterium *Hassallia* sp.

Torsten Neuhof,[†] Peter Schmieder,[‡] Karina Preussel,[†] Ralf Dieckmann,[†] Huong Pham,[†] Franz Bartl,[§] and Hans von Döhren*,[†]

Institut für Chemie, Fak. II, Technische Universität Berlin, 10587 Berlin, Germany, Forschungsinstitut für Molekulare Pharmakologie, 13125 Berlin, Germany, and Institut für Medizinische Physik und Biophysik, Charité-Universitätsmedizin Berlin, and Zentrum für Biophysik und Bioinformatik, Humboldt-Universität, 10117 Berlin, Germany

Received October 6, 2004

Hassallidin A (**1**), a new antifungal glycosylated lipopeptide, was isolated from an epilithic cyanobacterium collected in Bellano, Italy, identified as *Tolypothrix* (basionym *Hassallia)* species. Chemical, mass spectrometric, and spectroscopic analyses, including one- and two-dimensional NMR, were performed to determine an esterified eight-residue cyclic peptide linked with a carbohydrate and a fatty acid residue. Chiral GC-MS analysis revealed the occurrence of the nonproteinogenic amino acids D-*allo*-Thr, D-Thr, D-Tyr, D-Gln, and dehydroaminobutyric acid (Dhb) within the peptide moiety. The additional components of hassallidin A could be identified as α,β-dihydroxytetradecanoic acid (Dht) and mannose. This is the first report on a cyclic peptide of cyanobacterial origin that contains both a fatty acid and a carbohydrate moiety. Compound **1** exhibits antifungal activity against *Aspergillus fumigatus* and *Candida albicans* with MIC values of 4.8 μg/mL for both test organisms.

Cyanobacteria of various origins are an important source of new lead structures and drug improvement strategies.[1−4] Their ability to produce a broad spectrum of diverse structures in high quantity provides an immense pool of new potential bioactive agents.[5] Here we report the isolation and structure determination of a new antifungal compound from the cyanobacterium *Hassallia* sp. This compound represents a new structural type due to the co-occurrence of cyclic peptide, fatty acid, and carbohydrate moieties and, thus, with respect to a recent evaluation of the typology of cyanobacterial secondary metabolites,[6] represents a new molecular archetype. Antifungal peptides known so far are linear or cyclic peptides and lipopeptides, but lack glycosyl residues.[7]

Results and Discussion

The investigated cyanobacterial species was isolated in 2002 from epilithic cyanobacteria collected in Orrido Clough, Bellano, Italy, and identified as *Hassallia* sp. according to Geitler's characterization and taxonomy scheme.[8] Cells were grown for 30 days in modified BG-11 medium according to Welker[9] at 20 °C in 20 L flasks and were continuously illuminated and aerated. After filtration and lyophilisation, 4.3 g of dry material were obtained. The freeze-dried material was treated with MeOH to extract the active compound from the cyanobacterial biomass. After evaporation of solvent, the residue was eluted from a solid-phase extraction cartridge in preparation for HPLC. The biologically active fractions, collected on eight reversed-phase HPLC runs with an H_2O/MeCN gradient, were combined to yield 2.4 mg of hassallidin A (**1**). The new compound, hassallidin A (**1**), was isolated as a white amorphous powder. High-resolution electrospray Fourier transform ion cyclotron mass spectrometry (ESI-FTICR-MS) of hassallidin A revealed a quasi-molecular ion $[M + Na]^+$ at *m/z* 1404.67572 consistent with the calculated molecular formula of $[C_{62}H_{99}N_{11}O_{24}\ Na]^+$ (requires *m/z* 1404. 67618, relative mass error $\Delta_m = 0.33$ ppm). The signals from the UV spectrum detected at λ_{max} 226 nm (ϵ 5500), 278 nm (ϵ 880), and 265 nm (ϵ 700) predicted the occurrence of possible aromatic amino acid residues within the hassallidin A structure. The IR spectrum showed a strong absorption at 1740 cm^{-1}, predicting the presence of an ester group (lactone) within the molecular structure as well.

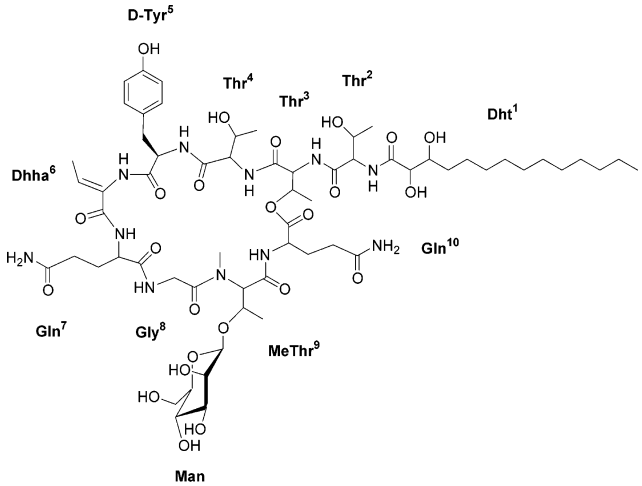

1

Amino acid analysis and quantification by enantiomer labeling of the total hydrolysate and chiral gas chromatography−mass spectrometry (GC-MS) gave the following relative molar concentrations: D-Tyr (1.00 ref.), D-Thr (0.96), L-Thr (0.88), D-*allo*-Thr (1.46), *N*-MeThr (1.01), D-Glu (0.82), L-Glu (0.90), Gly (1.02), and dehydroaminobutyric acid (Dhb) (one residue). Sugar analysis by GC-MS of the trimethylsilyl (TMS)-methylglycoside produced by acid hydrolysis and derivatization revealed the presence of only mannose. Additionally, by GC-MS analysis the fatty acid was identified as dihydroxytetradecanoic acid (Dht) by comparison of its native mass with that of the correspond-

* To whom correspondence should be addressed. Tel: ++49 30 314 22697. Fax: ++49 30 314 24783. E-mail: doehren@chem.tu-berlin.de.
[†] Technische Universität Berlin.
[‡] Forschungsinstitut für Molekulare Pharmakologie.
[§] Charité-Universitätsmedizin Berlin and Humboldt-Universität.

10.1021/np049671r CCC: $30.25
Published on Web 04/19/2005

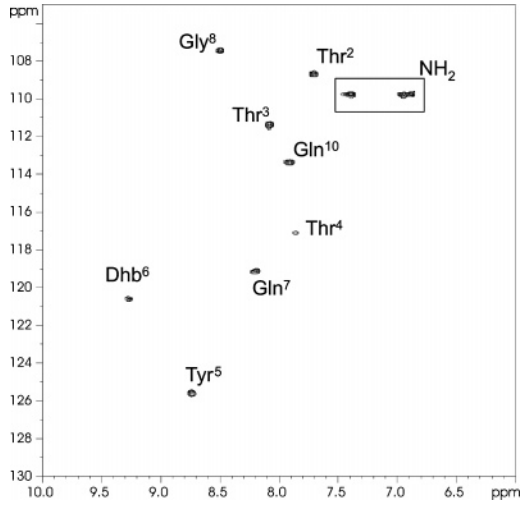

Figure 1. $^{1}H-^{15}N$-HSQC of hassallidin A in d_6-DMSO at 600 MHz. Eight correlations from amino protons to the directly attached nitrogen are visible, labeled according to the amino acid. In addition, the NH_2 groups of the two glutamines yield four signals.

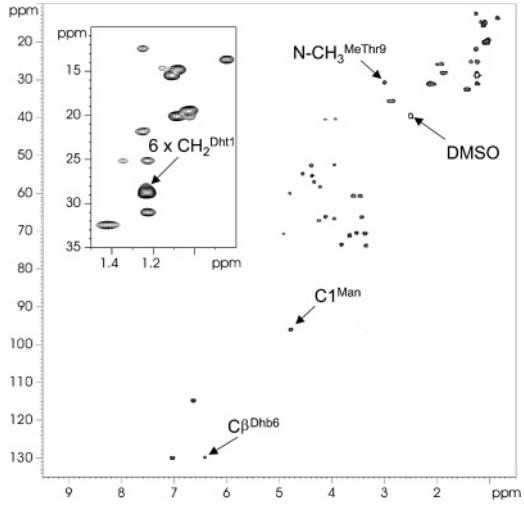

Figure 2. $^{1}H-^{13}C$-DEPT-HMQC of hassallidin A in d_6-DMSO at 600 MHz. Correlations from all protons directly attached to carbon are visible; those of methylene groups are negative and displayed in gray. In the region of the aromatic resonances (>110 ppm), the correlation of the tyrosine ring and the β-position of dehydroaminobutyric acid are visible. The anomeric carbon (C1) of the mannose is clearly visible at 96 ppm.

ing TMS-methyl derivative. The α- and β-position of the two hydroxy groups were determined by two-dimensional NMR experiments.

NMR spectroscopy was used to determine the constitution and arrangement of the individual "building blocks" independent from other methods. While a linear peptide of the size of hassallidin A would exhibit proton shifts near the random coil values, the good dispersion of the signals in the spectrum is in accordance with a cyclic peptide.

The analysis of the NMR data began with a comparison of the one-dimensional ^{1}H-spectrum with a set of heteronuclear spectra. An $^{1}H-^{15}N$ correlation spectrum (^{15}N-HSQC) showed eight signals from secondary amide protons and two pairs of signals from primary amide groups (Figure 1). An $^{1}H-^{13}C$ correlation spectrum (^{13}C-DEPT-HMQC, Figure 2) showed three signals in the range between 6 and 10 ppm as the only carbon-bound protons in that region. The integral of the broad proton signals around 9.17 ppm indicated two protons close to each other. Only the signal at 9.18 ppm was found in the $^{1}H-^{15}N$ correlation. The signal at 9.16 ppm therefore indicated a proton bound neither to ^{15}N nor to ^{13}C, most likely an OH at the aromatic ring of tyrosine.

Further analysis of the carbon-bound protons was based on the HMQC and on a DEPT-HMQC and an HQQC. The latter showed only signals from methyl groups, while the former indicated the different multiplicities of the carbon spectra by an inverted sign for methylene groups. Seven methyl groups could be detected, one of them at chemical shifts of 2.99 ppm (^{1}H) and 30.64 ppm (^{13}C), which are typical values for *N*-methyl groups. In addition 18 CH groups were found, one with a chemical shift of 95.95 ppm, typical for anomeric signals of hexose moieties. The remaining 11 signals were from CH_2 groups. Some of those signals, however, clearly represented more than one carbon atom. In particular, the region between 1.15 and 1.5 ppm (^{1}H chemical shift) showed five CH_2 and one CH_3 group (see inset in Figure 2). The integration of the one-dimensional spectrum, however, indicated the presence of 23 protons. The strong peak at 1.23/28.75 ppm thus had to contain six CH_2 groups, which was confirmed by inspecting a one-dimensional carbon spectrum. Since no individual assignment is possible, all carbons are given with the same chemical shift in Table 1. Several signals from the one-dimensional ^{1}H spectrum had no corresponding signals in the HMQC and were thus most likely OH protons, since no exchange broadening was observable.

The next step of the identification of individual residues in hassallidin A focused on proteinogenic amino acids. The analysis was initially based on heteronuclear spectra: The HMQC was combined with an HMQC-COSY and HMQC-TOCSYs with different mixing times as well as an HMBC. The results obtained from those spectra were subsequently confirmed by using homonuclear spectra, in particular a DQF-COSY and TOCSY spectra of several mixing times. On the basis of those spectra, the following amino acids could be identified: glycine, tyrosine, two glutamines, and three threonines. Additional signals typical for another threonine were also found, but the amino proton was lacking. A correlation of the methyl group at 2.99/30.64 ppm ($^{1}H/^{13}C$) to the C^{α} of that threonine in the HMBC confirmed that the fourth threonine was methylated at the nitrogen. Two of the threonines did not show signals of OH protons. Since all other OH protons were visible, these two threonine side chains were most likely chemically modified.

The next step was the assignment of the remaining resonances to moieties other than proteinogenic amino acids. The spectra indicated that the signal at 6.41/130.12 ppm ($^{1}H/^{13}C$) was coupled to one of the methyl groups, because no other protons seemed to belong to the same spin system. On the basis of correlations found in the HMBC, the signals could be linked to the amino proton at 9.18 ppm that did not show any correlation in homonuclear spectra and to a further, quaternary carbon at 129.72 ppm. In conjunction, the signals added up to a dehydroaminobutyric acid residue (Dhb), which could subsequently be confirmed in a homonuclear NOESY spectrum. Since this spectrum showed a correlation from the amino proton to the methyl group but not to the olefinic proton, Dhb had to be in the *Z*-configuration.

Resonances in the region between 60 and 75 ppm in the ^{13}C NMR spectrum and around 3.5 ppm in the ^{1}H NMR spectrum were all identified as signals from a hexose moiety. Correlations to the resonance at 95.95 ppm in carbon were also found. The type of hexose could not be determined from the NMR spectra. All protons of the hexose showed correlations to OH protons in the

Table 1. ^{1}H and $^{13}C/^{15}N$ NMR Data for Hassallidin A in d_6-DMSO

component	position	δ_H (ppm)	$\delta_{C/N}$ (ppm)	component	position	δ_H (ppm)	$\delta_{C/N}$ (ppm)
Dht-1	14	0.84	13.64	Dhb-6	HN	9.18	120.60
	13	1.25	21.80		α		129.72
	12	1.23	30.96		*β*	6.41	129.65
	11[a]	1.23	28.75		*γ*	1.23	12.41
	10[a]	1.23	28.75		CO		163.37
	9[a]	1.23	28.75	Gln-7	HN	8.10	119.11
	8[a]	1.23	28.75		α	3.94	52.41
	7[a]	1.23	28.75		*β*	1.97/1.90	25.78
	6[a]	1.23	28.75		*γ*	2.13	31.03
	5	1.35/1.22	25.11		CO		n.d.
	4	1.42	32.41		*γ*-CO		174.49
	3	3.65	71.11		NH_2	7.31/6.80	109.72
	2	3.81	73.47	Gly-8	HN	8.40	107.41
	2-OH	5.49			a	4.11/3.93	40.37
	3-OH	4.38			CO		169.88
	CO		176.50	MeThr-9	NCH_3	2.99	30.64
Thr-2	HN	7.62	108.67		α	4.79	59.96
	α	4.33	56.93		*β*	4.23	67.10
	β	4.11	66.09		*γ*	1.08	14.79
	γ	1.03	19.48		CO		n.d.
	OH	5.12		Man	1	4.77	95.95
	CO		169.88		2	3.52	70.34
Thr-3	HN	7.98	111.33		3	3.36	70.47
	α	4.54	54.77		4	3.43	66.16
	β	4.91	70.64		5	3.34	73.84
	γ	1.11	15.47		6	3.45/3.58	60.57
	CO		n.d.		2-OH	4.67	
Thr-4	HN	7.78	117.09		3-OH	4.49	
	α	4.21	58.28		4-OH	4.62	
	β	3.95	66.56		6-OH	4.24	
	γ	1.09	20.08	Gln-10	HN	7.83	113.36
	OH	5.20			α	4.38	52.54
	CO		n.d.		*β*	1.87	28.07
Tyr-5	HN	8.64	125.58		*γ*	2.08/2.13	31.03
	α	4.37	55.24		CO		n.d.
	β	2.90/2.83	35.50		*γ*-CO		174.22
	1		126.96		NH_2	7.30/6.86	109.73
	2/6	7.02	130.12				
	3/5	6.63	115.00				
	4		155.92				
	OH	9.16					
	CO		170.22				

[a] Due to overlap in the NMR, spectra cannot be individually assigned.

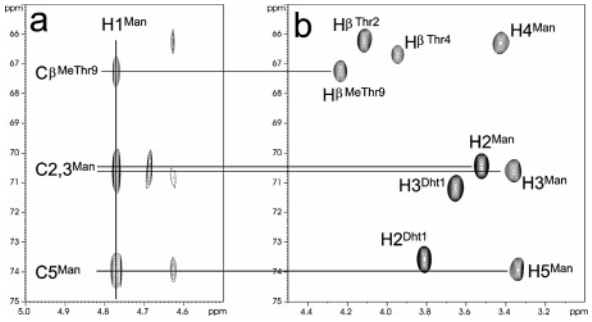

Figure 3. Region of the $^{1}H-^{13}C$-HMBC (a) and the $^{1}H-^{13}C$-HMQC (b) of hassallidin A in d_6-DMSO at 600 MHz. In the HMBC correlations of the H1 proton within the mannose (anomeric proton) via $^{2}J_{HC}$ (reaching C2) and $^{3}J_{HC}$ (reaching C3 and C5) are visible. In addition the correlation to the C*β* of MeThr9 proves the attachment of the mannose to the side chain of MeThr9 via its anomeric position.

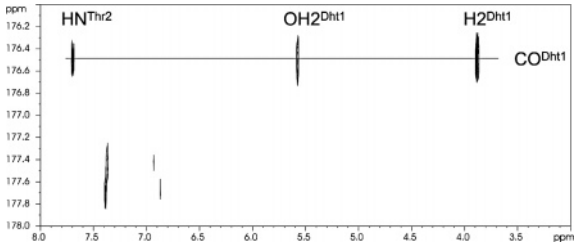

Figure 4. Region of the $^{1}H-^{13}C$-HMBC of hassallidin A in d_6-DMSO at 600 MHz. Correlations of the side chain carbonyl carbons of the two glutamines are visible as well as those of the carbonyl of the fatty acid (Dht1). The latter shows correlation to the OH and the proton attached to the second carbon atom in the fatty acid chain. More importantly, a correlation to the amino proton of Thr2 is visible, proving the attachment of Dht1 to the nitrogen of Thr2.

HMQC-COSY spectrum except for the anomeric carbon. This indicated that the hexose is linked to the peptide via its anomeric carbon. Figure 3 shows a region of the HMBC. The proton attached to the anomeric carbon of the hexose ($H1^{Man}$) showed a correlation to the C*β* of Thr9 in the HMBC, thus confirming the link of the hexose to the threonine that was previously identified as an *N*-methylated threonine.

Two correlations in the HMQC, at 3.81/73.05 ppm ($^{1}H/^{13}C$) and 3.65/71.09 ppm ($^{1}H/^{13}C$), showed correlations to OH protons and a coupling between each other in the HMQC-COSY. The signal at 3.65/71.09 ppm ($^{1}H/^{13}C$) showed a correlation to the bulk of CH_2 groups around 1.3 ppm. HMQC-TOCSY and HMBC spectra exhibited many correlations within these carbons and to the methyl group at 0.84/13.65 ppm ($^{1}H/^{13}C$). Altogether this indicated the presence of a long chain of 13 protonated carbon atoms, the first two having an OH group attached, the final one being a methyl group. Figure 4 shows a region of the HMBC with correlations from the proton attached to the first carbon of that long chain, the OH attached to it, and

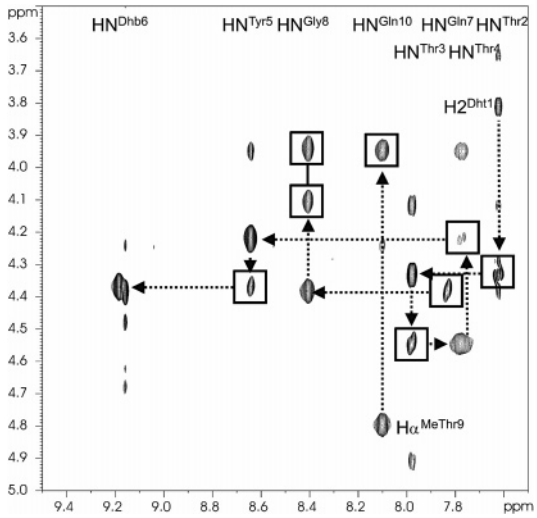

Figure 5. Fingerprint region from the NOESY of hassallidin A in d_6-DMSO at 600 MHz. Correlations from the amino protons to the H^{α} protons are visible. Intraresidue correlations are marked with rectangles. The dotted lines indicate the "sequential walk" linking the individual amino acids together. Two links are not depicted (Dhb6 to Gln7 and Gly8 to MeThr9) since the relevant correlations are outside of the spectral region shown here.

the amino proton of Thr2 all attached to the same carbonyl carbon at 176.5 ppm. This indicates that the carbonyl carbon is the first carbon in a C_{14}, α,*β*-dihydroxytetradecanoic acid chain (Dht) that is attached to the nitrogen of the first threonine in the chain.

Since the HMBC did not show enough correlations from amino protons to carbonyl carbons, the amino acid sequence was established on the basis of sequence-specific assignment using NOESY and TOCSY spectra. Intraresidue peaks in the NOESY were identified by comparison with the TOCSY spectrum. Then a "sequential walk" was performed as shown in Figure 5. Correlations between amino protons and both H^{α} and H^{β} protons confirmed the sequential connectivities. Partial sequences could thus be established: the first was Thr-Thr-Thr-Tyr-Dhb, the second Gln-Gly, and the third MeThr-Gln. Between the three chains, the missing H^{α} in Dhb and the missing amino proton in MeThr prevented use of the conventional strategy. Sequential correlations between amino proton of Gln7 and the H^{β} proton of Dhb as well as the *N*-methyl group of MeThr9 and the H^{α} protons of Gly8, however, closed the two gaps. A sequence Thr-Thr-Thr-Tyr-Dhb-Gln-Gly-MeThr-Gln could therefore be established.

The remaining question was the missing OH proton of Thr3. Since the peptide is obviously cyclized via a lactonic bond, a cyclization via the side chain of Thr3 is likely. A complete list of all ^1H, ^{13}C, and ^{15}N chemical shifts and the assignment of hassallidin A is given in Table 1.

Deduced data of the hassallidin A constitution obtained by NMR and acid hydrolysis were confirmed by MALDI-TOF post-source decay (PSD) and ESI-$MS^{(n)}$ experiments. The reflector mode MALDI-TOF mass spectrum performed with delayed extraction (DE) showed a positive ion signal at *m/z* 1404.8, identified as a sodium-ion associated monoisotopic peak $[M + Na]^+$ of hassallidin A. In addition there was a second significant mass signal at *m/z* 1220.7 in the reflector mode, corresponding to a protonated mass signal of hassallidin A without mannose (mass loss of *m/z* 162). Additional signals in the reflector mode during analysis of glycopeptides are caused by a rapid formation of ions within the ion source, which is known as in-source decay (ISD).[10] Influenced by different parameters, such as matrix, compound residues, and the use of delayed extraction,[11] ISD fragments can often be observed in the same spectrum when recorded with delayed extraction TOF instruments operated in the reflector mode. By the use of the ISD ion as precursor ion in the PSD mode, subsequence information of the lipopeptide moiety confirmed the predicted amino acid sequence of the NMR experiments. Interpretations of fragment mass signals are listed in Table 2. By using the collision cell in the low mass range of the PSD mode, immonium ions ($^+NH_2{=}CH{-}R$) were released to provide further information about the present amino acids. Immonium ion signals (rel int %) for Thr *m/z* 74 (14), MeThr *m/z* 88 (20), Gln *m/z* 101 (13), Gly *m/z* 30 (2), Tyr *m/z* 136 (4), and Dhb *m/z* 56 (6) were detected.

Table 2. MALDI-TOF-PSD Fragment Ions of the Hassallidin A Lipopeptide Moiety

ion composition[a]	(*m/z*)/int(%)
M − [*m/z* 243 (Dht)]	977/(2)
M − [*m/z* 243 (Dht) − *m/z* 101 (Thr)]	876/(8)
M − [*m/z* 128 (Gln)]	1092/(11)
M − [*m/z* 128 (Gln) − *m/z* 57 (Gly)]	1035/(5)
M − [*m/z* 128 (Gln) − *m/z* 57 (Gly) − *m/z* 115 (MeThr)]	920/(33)
M − [*m/z* 128 (Gln) − *m/z* 57 (Gly) − *m/z* 115 (MeThr) − *m/z* 128 (Gln)]	792/(7)
M − [*m/z* 83 (Dhb) − *m/z* 128 (Gln) − *m/z* 57 (Gly) − *m/z* 115 (MeThr) − *m/z* 128 (Gln)]	709/(2)
M − [*m/z* 163 (Tyr) − *m/z* 83 (Dhb) − *m/z* 128 (Gln) − *m/z* 57 (Gly) − *m/z* 115 (MeThr) − *m/z* 128 (Gln)]	546/(3)
M − [*m/z* 101 (Thr) − *m/z* 163 (Tyr) − *m/z* 83 (Dhb) − *m/z* 128 (Gln) − *m/z* 57 (Gly) − *m/z* 115 (MeThr) − *m/z* 128 (Gln)]	445/(6)
[*m/z* 57 (Gly) − *m/z* 115 (MeThr) + H]$^+$	173/(33)
[*m/z* 83 (Dhb) − *m/z* 128 (Gln) + H]$^+$	212/(4)
[*m/z* 57 (Gly) − *m/z* 115 (MeThr) − *m/z* 128 (Gln) + H]$^+$	301/(48)
[*m/z* 57 (Gly) − *m/z* 115 (MeThr) − *m/z* 128 (Gln) − *m/z* 83 (Dhb) + H]$^+$	384/(38)
[*m/z* 128 (Gln) − *m/z* 57 (Gly) − *m/z* 115 (MeThr) − *m/z* 128 (Gln) + H]$^+$	429/(21)

[a] M = [*m/z* 1381 + H]$^+$ − mannose [*m/z* 162] = [*m/z* 1219 + H]$^+$.

Fragmentation patterns of the protonated monoisotopic peak at *m/z* 1382 for hassallidin A were also studied using ESIMS/MS experiments. Formation of one first-generation fragment ion was accompanied by a loss of *m/z* 162 for mannose to result in a mass signal of *m/z* 1220. The following daughter-fragment ion series of the first-generation ion M were detected and interpreted as follows: *m/z* 1092: M − [*m/z* 128 (Gln)], *m/z* 920: M − [*m/z* 128 (Gln) − *m/z* 57 (Gly) − *m/z* 115 (MeThr)], and *m/z* 792: M − [*m/z* 128 (Gln) − *m/z* 57 (Gly) − *m/z* 115 (MeThr) − *m/z* 128 (Gln)].

The antifungal activity of hassallidin A was verified by minimum inhibitory concentration (MIC) data in a serial dilution test. MIC values for hassallidin A against *Candida albicans* and *Aspergillus fumigatus* were found to be 4.8 μg/mL for both test organisms, using RPMI-1640 medium. Hassallidin A also shows precise antifungal activity when tested in disk diffusion assays (10 μg in 30 μL of 50% MeOH per disk) on malt agar plates against *Aspergillus fumigatus, Aspergillus niger*, *Ustilago maydis*, *Penicillium* sp.**,** *Fusarium sambucium, Candida albicans,* and *Candida glabrata*. No activities were observed by using *Bacillus subtilis, Streptomyces versicolor*, or *Escherchia coli* in disk diffusion assays on LB-agar plates with 10 μg of hassallidin A in 30 μL of 50% MeOH per disk.

Experimental Section

General Experimental Procedures. UV spectra were recorded on a Shimadzu UV-160 spectrophotometer. The IR spectra were recorded using a Bruker IFS 66v/S Fourier transform infrared spectrometer (FTIR).

NMR spectra were recorded at 600 MHz (^{1}H frequency) using Bruker DRX spectrometers. One milligram of hassallidin A was dissolved in 550 μL of d_6-DMSO, yielding a concentration of 1.4 mM. Most spectra were recorded using a 5 mm triple-resonance probe (H,C,N) equipped with three-axis self-shielded gradients. A carbon one-dimensional spectrum was recorded using a 5 mm dual-resonance probe (H,C). The ^{13}C-HMBC and the ^{15}N-HSQC were recorded using a cryogenic 5 mm triple-resonance probe (H,C,N) equipped with one-axis self-shielded gradients. One-dimensional proton and carbon spectra were recorded with 32 and 100 000 scans using 8K and 128K data points, respectively. All homonuclear two-dimensional spectra (DQF-COSY,[12] NOESY,[13] TOCSY[14,15]) were recorded using 2048 × 512 complex data points. The DQF-COSY was recorded using 32 scans; the TOCSYs were recorded using 16 scans and mixing times of 30, 60, and 120 ms; and the NOESY was recorded using 32 scans and a mixing time of 100 ms. Most heteronuclear two-dimensional spectra were recorded using 512 × 256 complex data points. The ^{13}C-HMQC[16] and the ^{13}C-DEPT-HMQC[17] were recorded using 96 scans; the ^{13}C-HMQC-TOCSY[18] spectra were recorded with 160 and 256 scans using mixing times of 20 and 120 ms, respectively. The ^{13}C-HMQC-COSY[19] was recorded with 512 × 384 complex data points using 512 scans. The ^{13}C-HQQC[20] was recorded with 512 × 64 complex data points using a reduced spectral width and 96 scans. All the above heteronuclear spectra were recorded using a BIRD pulse for suppression of protons bound to ^{12}C.[21] A gradient-^{13}C-HMBC[22] was recorded with 2048 × 512 complex data points using 176 scans, and the ^{15}N-HSQC[23] was recorded with 512 × 64 complex data points using 360 scans.

The GC-MS analyses were performed on an Agilent 6890/5793 MSD system. Mass spectra were obtained on a PerSeptive Biosystems Voyager-DE PRO MALDI-TOF mass spectrometer and on a Bruker esquire 2000 LC-MS system equipped with an electrospray source. The high-resolution ESI-FTICR mass spectrum was obtained on a Finnigan ThermoQuest device. HPLC separations were performed on a Waters 515 system coupled to a photodiode array detector and autosampler. The optical density was measured with a Tecan-Genios microplate reader at 595 nm.

Organism and Culture Conditions. *Hassallia* sp. B02-07 was isolated in 2002 from epilithic cyanobacteria, which were collected in Orrido Clough, Bellano, Italy. The sample was preincubated in BG-11 medium modified by Welker:[9] [$NaNO_3$ (10 mM), K_2HPO_4 (1 mM), $MgSO_4 \times 7H_2O$ (0.7 mM), $CaCl_2$ (0.2 mM), Na_2CO_3 (0.2 mM), Na_2EDTA (0.1 mM), citric acid (0.1 mM), $FeCl_3 \times 6H_2O$ (0.02 mM) containing 1 mL/L medium trace elements additional with thiamine HCl (300 nM), biotin (2 nM), and cyanocobalamin (0.4 nM)] and individualized by plating cultural solution on agar plates (1% agarose in BG-11 medium). For mass cultivation the strain grew in 20 L polycarbonate bottles with the modified BG-11 medium and permanent sterile aeration at room temperature. The cultures were constantly illuminated by daylight lamps (Philips TLD 58W/840). Cyanobacterial material was harvested by percolation after 30 days, to give yields of lyophilized cells from 4.3 g.

Extraction and Isolation. A portion of 4 g of freeze-dried cyanobacterial biomass was extracted with 75% MeOH (500 mL) for 3 h and was separated by centrifugation. After removal of solvent in a vacuum rotary evaporator at 50 °C, the crude extract (16 mg) was taken up in 20 mL of 90% MeOH and eluted from a solid-phase extraction cartridge (Waters Oasis HLB Extraction Cartridge) with 75% MeOH, filtrated through a 0.22 μm filter (Roth Rotilabo), and subjected to HPLC in eight portions [Waters Spherisorb S5 ODS2, 10 × 250 mm column; mobile phase: solvent A: H_2O/formic acid (0.05%), solvent B: acetonitrile/formic acid (0.05%); 3 mL/min; UV detection at 220 nm]. The following gradient was applied: solvent B from 30% to 35% in 10 min, 35% to 70% in 30 min, 70% to 100% in 4 min, isocratic 6 min. The fractions that exhibited antifungal activity eluted at 23−24 min. Fractions from eight HPLC runs were collected and combined. After removing the solvent under reduced pressure, 2.4 mg of purified hassallidin A was obtained.

Hassallidin A (1): white, amorphous solid; UV (MeOH) λ_{max} 226 nm (ϵ 5500), 278 nm (ϵ 880), 265 nm (ϵ 700); IR ν_{max} (film) 3448, 3343, 3282, 3080, 2927, 2853, 1740, 1658, 1617, 1543, 1530, 1527, 1453, 1384, 1268, 1240, 1232, 1172, 1128, 1091, 1067 cm^{-1}; ^{1}H and ^{13}C NMR, see Table 1; HR-ESI-FTICR-MS *m/z* $[M + Na]^+$ 1404.67572 (calcd for $[C_{62}H_{99}N_{11}O_{24}Na]^+$ 1404.67618, relative mass error $\Delta_m = 0.33$ ppm).

MS Analysis. Mass spectral analyses were performed on a matrix-assisted laser desorption/ionization time-of-flight (MALDI-TOF) and a liquid chromatography-electrospray-ionization (LC-ESI) mass spectrometer.

Sample application for MALDI-TOF measurements was carried out directly on sample plates with a mixture of 1 μL of matrix (saturated 2,5-dihydroxybenzoic acid in 50% acetonitrile, 0.3% TFA) and 1 μL of a 50% MeOH solution containing about 0.2 μg of hassallidin A.

The monoisotopic mass of hassallidin A was determined in positive ion reflector mode by using delayed extraction (DE). To obtain additional structural information, the fragmentation pattern was recorded using the post-source decay (PSD) modus and stepwise lowering the reflector voltage. Below *m/z* 300 air was introduced into the collision cell, which increased the number of small fragments and immonium ions. The liquid chromatography system of the LC-ESI-MS was performed with an Agilent Zorbax SB-C_{18} 5 μm, 4.6 × 150 mm column [mobile phase: solvent A: H_2O/TFA (0.02%), solvent B: acetonitrile/TFA (0.02%), 0.5 mL/min; UV detection at 220 nm]. The gradient was solvent B from 20% to 100% in 20 min and isocratic 5 min. The desired mass signal appeared at 11.5−13.0 min. The injection volume was 4 μL (about 80 pmol of hassallidin A) of a 50% MeOH solution. The MS spectra were generated on a dual octopole ion trap mass spectrometer operated in positive ion mode and fitted with an atmospheric pressure electrospray-ionization sample introduction device. Fragmentation experiments were performed by automatic $MS^{(n)}$ technique.

Chiral Amino Acid Analysis. Approximately 50 nM of sample was hydrolyzed in 200 μL of 6 N HCl (110 °C/24 h). The dry hydrolysate was derivatized to the *N*-(*O*-)trifluoroacetyl/ethyl ester and analyzed by GC-MS (Agilent 6890/5973 MSD) using a 20 m × 0.25 mm Lipodex E/PS255 (30:70) capillary column. Quantitative analysis was performed by enantiomer labeling.[24]

Sugar and Fatty Acid Analysis. The sample was heated at 70 °C for 16 h with 0.65 N HCl/abs MeOH. Excess methanol was evaporated off. The dry residue was treated with *N*,*O*-bis(trimethylsilyl)trifluoroacetamide (BSTFA)/acetonitrile (1:1) (60 °C/30 min), and the derivatized sugar and fatty acid were analyzed directly by GC-MS on a DB-5 capillary (J + W, Folson).

Antifungal Assay. Determination of the minimum inhibitory concentration (MIC) of hassallidin A for *Aspergillus fumigatus* and *Candida albicans* was performed in a microdilution assay. For each fungus six testing wells of a microtiter plate were prepared with 240 μL of medium (Sigma RPMI-1640), 10 μL of inoculum suspension, and 50 μL of fungicide solution (50% MeOH) of different concentrations. The inoculum preparation was carried out by guidelines of NCCLS.[25] The fungicide solution preparation took place in a series of 2-fold dilutions from a stock solution of 92 μg/mL starting with 4.6 μg/50 μL down to 0.14 μg/50 μL. One well was prepared without antifungal agent for unhindered growth as control. The microtiter plates were incubated for *Candida albicans* and *Aspergillus fumigatus* at 35 °C for 24 and 48 h, respectively. Tests were run in triplicate. Inhibition of growth was assessed by comparing the fungal growth of the test samples with the control well by determination of optical density at 595 nm in a microplate reader. The concentration of the well at highest

dilution that was still free from growth was assigned the minimum inhibitory concentration (MIC in μg/mL).

Acknowledgment. This research was supported by the Deutsche Forschungsgemeinschaft [DFG: DO 270/10-3]. Thanks to T. Schmiederer, G. Nicholson, and R. D. Süssmuth (Mikrobiologisches Institut, Universität Tübingen, 72076 Tübingen, Germany) for performing the GC-MS analysis, Bio-Mar GbR (Merowinger Platz 1a, 40225 Düsseldorf, Germany) for further LC-MS experiments, and M. v. Löwis (Humboldt-Universität, Institut für Chemie, 12489 Berlin, Germany) for the HR-FTICR-MS data. Also thanks to B. Hube (Robert-Koch-Institut, NG4, 13353 Berlin, Germany) for providing the fungal strains.

References and Notes

(1) Blom, J. F.; Bister, B.; Bischoff, D.; Nicholson, G.; Jung, G.; Süssmuth, R. D.; Jüttner, F. *J. Nat. Prod.* **2003**, *66*, 431−434.
(2) Burja, A. M.; Banaigs, B.; Abou-Mansour, E.; Burgess, J. G.; Wright, P. C. *Tetrahedron* **2001**, *57*, 9347−9377.
(3) Lesser, M. P.; Mazel, C. H.; Gorbunov, M. Y.; Falkowski, P. G. *Science* **2004**, *13*, 997−1000.
(4) Proksch, P.; Edrada, R. A.; Ebel, R. *Appl. Microb. Biotechnol*. **2002**, *59*, 125−134.
(5) Namikoshi, M.; Rinehart, K. L. *J. Ind. Microb. Biotechnol.* **1996**, *17*, 373−384.
(6) Guyot, M.; Dore, J. C.; Devillers, J. *SAR QSAR Environ. Res.* **2004**, *15* (2), 101−114.
(7) De Lucca, A. J.; Walsh, T. J. *Antimicrob. Agents Chemother*. **1999**, *43*, 1−11.
(8) Geitler, L. In *Synoptische Darstellung der Cyanophyceen in morphologischer und systematischer Hinsicht*; Beih. Bot. Centralbl. 1932; Chapter 2, pp 163−324.
(9) Welker, M.; Christiansen, G.; von Döhren, H. *Arch. Microbiol.* **2004**, *182*, 288−298.
(10) Harvey, D. J. *Mass Spectrom. Rev.* **1999**, *18*, 349−451.
(11) Takayama, M. *J. Am. Soc. Mass Spectrom.* **2001**, *12* (4), 420−7.
(12) Piantini, U.; Sorensen, O. W.; Ernst, R. R. *J. Am. Chem. Soc.* **1982**, *104*, 6800−6801.
(13) Jeener, J.; Meier, B. H.; Bachmann, P.; Ernst, R. R. *J. Chem. Phys.* **1979**, *71*, 4546−4553.
(14) Braunschweiler, L.; Ernst, R. R. *J. Magn. Reson.* **1983**, *53*, 521−528.
(15) Bax, A.; Davis, D. G. *J. Magn. Reson.* **1985**, *65*, 355−360.
(16) Bax, A.; Griffey, R. H.; Hawkins, B. L. *J. Am. Chem. Soc.* **1983**, *105*, 7188−7190.
(17) Kessler, H.; Schmieder, P.; Kurz, M. *J. Magn. Reson.* **1989**, *85*, 400−405.
(18) Lerner, L.; Bax, A. *J. Magn. Reson.* **1986**, *69*, 375−380.
(19) Clore, G. M.; Bax, A.; Wingfield, P.; Gronenborn, A. M. *Febs Lett.* **1988**, *238*, 17−21.
(20) Kessler, H.; Schmieder, P.; Kock, M.; Reggelin, M. *J. Magn. Reson.* **1991**, *91*, 375−379.
(21) Bax, A.; Subramanian, S. *J. Magn. Reson.* **1986**, *67*, 565−569.
(22) Bax, A.; Summers, M. F. *J. Am. Chem. Soc.* **1986**, *108*, 2093−2094.
(23) Bodenhausen, G.; Ruben, D. J. *Chem. Phys. Lett.* **1980**, *69*, 185−189.
(24) Frank, H.; Nicholson, G. J.; Bayer, E. *J. Chromatogr.* **1978**, *167,* 187−196.
(25) In *Approved Standard, NCCLS document M38-A*; National Committee for Clinical Laboratory Standards, 1998; Vol. 22, Number 16.

NP049671R